Thermochimica Acta, 80 (1984) 11–21
Elsevier Science Publishers B.V., Amsterdam – Printed in The Netherlands

STUDIES ON THE REDUCTION OF THE Fe_2O_3–MoO_3 SYSTEM AND ITS INTERACTION WITH SYNTHESIS GAS (CO + H_2)

G.C. MAITI *, R. MALESSA and M. BAERNS

Lehrstuhl für Technische Chemie, Ruhr Universität Bochum, Postfach 102148, D-4630 Bochum (F.R.G.)

(Received 19 March 1984)

ABSTRACT

The structural changes of iron–molybdenum mixed oxide systems during calcination and reduction were studied. The oven-dried precipitated mass contains excess molybdenum as polymolybdic ions, which is transformed into $Fe_2(MoO_4)_3$ and MoO_3 on heat-treatment of the sample above 400 °C. The reduction of $Fe_2(MoO_4)_3$ proceeds through the formation of $FeMoO_4$ and $FeMoO_3$. On complete reduction, it gives a mixed crystal of iron and molybdenum. MoO_3 is also simultaneously reduced to elemental molybdenum through the formation of MoO_2 as an intermediate oxide.

The interaction of the reduced mass with synthesis gas indicates that the iron–molybdenum mixed crystal is active for the hydrogenation of CO molecules. This mixed lattice is also stable towards the carburization process under synthesis gas.

INTRODUCTION

The major problem for a Fischer–Tropsch synthesis is the rapid deactivation of the catalytic mass due to the presence of sulphur compounds in the synthesis gas, produced by coal gasification [1–4]. In this respect, several attempts have been made to develop a more stable catalyst consisting of MoO_3, which possesses a greater sulphur-tolerance. So far, mainly the development of supported molybdenum catalysts have been reported [5–8]. The present study investigates the reducibility of Fe_2O_3–MoO_3 mixed oxide systems and their catalytic activity for the hydrogenation of CO. Iron oxide is widely used as a suitable active precursor for the hydrogenation of CO [1,9,10]. However, elemental iron is susceptible to the sulphur impurities. MoO_3 has been incorporated with the iron oxide mass in order to improve the sulphur tolerance properties of the catalytic mass. Although the nature of the reduction of $Fe_2(MoO_4)_3$ to $Fe(MoO_4)$ has been widely studied [11–15],

* Present address: Physical Research Wing, Project and Development India Ltd., Sindri 828122, India.

0040-6031/84/$03.00

information on its further reduction to the elemental stage is limited [16–18]. The latter reduction process seems to be necessary for the enhancement of catalytic activity in the hydrogenation of CO.

EXPERIMENTAL

Materials and methods

A mixed oxide consisting of iron and molybdenum was prepared by precipitation from an aqueous solution of $(NH_4)_6Mo_7O_{24} \cdot 4\ H_2O$ (0.025 M) and $Fe(NO_3)_3 \cdot 9\ H_2O$ (0.15 M). The pH of the mixture was maintained at 1.8 ± 0.1. After mixing the solution for 2 min the precipitated mass was separated by centrifuging for 10 min (3000 min^{-1}). The precipitated mass was thoroughly washed several times in distilled water and oven-dried at 120 °C under vacuum. This sample will be referred to as sample A.

Another sample (sample B) was prepared by the simple mechanical mixing of Fe_2O_3 and MoO_3 in a mortar ball mill for 1 h. Fe_2O_3 was obtained by calcining the precipitated hydroxide mass at 400 °C for 10 h. MoO_3 was obtained by the thermal decomposition of $(NH_4)_6Mo_7O_{24} \cdot 4\ H_2O$ at 300 °C for 2 h. The mechanical mixture consisted of 1 mol of Fe_2O_3 and 3 mol of MoO_3. All the chemicals used were pro analysis grade. Sample A was used for studying the structural changes during the calcination process. Samples A and B, and pure MoO_3 were used to study the nature of the reduction process. Hydrogenation of CO was examined for the reduced samples, obtained from samples A and B, and MoO_3.

Thermoanalytical measurements were performed with a controlled-atmosphere DSC instrument (DuPont DTA-990). The sample and α-Al_2O_3, used as a standard, were placed in two different gold caps. During calcination in argon atmosphere and reduction with hydrogen, the temperature was increased by 10 °C min^{-1}. For the synthesis experiment a gas mixture of CO and H_2 was used at 10 bar ($P^0_{H_2} = 6.3$ bar; $P^0_{CO} = 3.4$ bar). The total gas flow was 50 ml min^{-1} and was controlled with an electro flowmeter (Brooks 4250-HA 281 EO). Pre-reduced samples were used for the synthesis experiment. The reduction of the samples was carried out at 600 °C for 50 h under hydrogen. A sample of about 15 mg was used in each experiment.

X-ray diffraction patterns of the samples were recorded by a Guinier camera applying crystal-reflected monochromatic FeK_{α_1} radiation (operating conditions: 50 kV; 20 mA). Silicon was used as an internal standard for the correction of the angles derived from the diffraction lines and of the instrumental broadening for the crystallite size measurements. The crystal phase composition of the samples was determined by comparing the measured *d*-spacings with standard ASTM values [19]. The lattice parameter values were determined from correction θ values using a suitable computer

program. To avoid any interaction between the reduced samples and ambient atmosphere for X-ray studies, the catalysts were always handled under inert gas and coated with colloid ion. It was confirmed that no oxidation of the samples occurred during handling.

IR-spectra were recorded with a Perkin-Elmer 225 spectrophotometer using 3-mg samples admixed to 300 mg KBr in an agate mortar and then pelletized in the usual way in an evacuated 13 mm ϕ die. The samples were dried for 12 h at 120 °C prior to preparing the pellets.

In sample A, molybdenum was estimated by the gravimetric method by precipitating with $Pb(NO_3)_3$ solution and, after the separation of molybdenum, iron was precipitated with NH_4OH and also estimated gravimetrically. The chemical analysis gave the elemental concentration ratio of iron and molybdenum as 33.8 and 66.2%, respectively, in the case of sample A.

RESULTS

Calcination

The calcination of the precipitated mass was carried out under an argon atmosphere. The DSC curve is shown in Fig. 1.

The DSC curve shows two endothermic peaks at 120 and 250 °C. The endothermic process is followed by an exothermic peak at 373 °C, which is a doublet.

The X-ray diffraction results are shown in Table 1. XRD studies indicate that the oven-dried mass at 120 °C is poorly crystalline. On calcining the sample at 250 °C, however, the formation of the $Fe_2(MoO_4)_3$ phase has been observed in the XRD pattern. The X-ray diffraction pattern does not indicate any free MoO_3 phase at 250 °C. It indicates the formation of a separate MoO_3 phase along with the $Fe_2(MoO_4)_3$ phase, on heat treatment

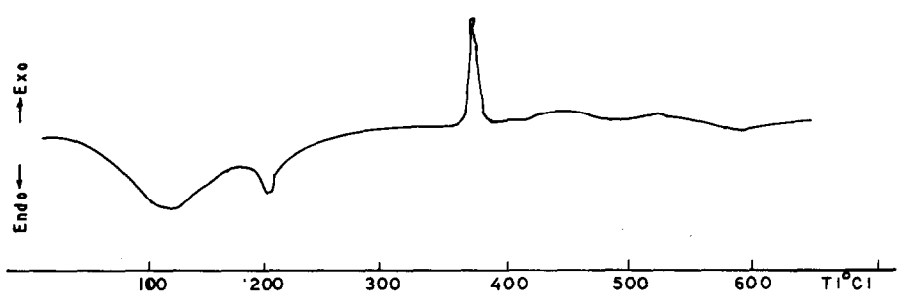

Fig. 1. DSC curve of precipitated iron–molybdenum mixed oxide sample under argon atmosphere.

TABLE 1

Crystal phase composition of samples A and B

Temp. (°C)	Calcination duration (h)	Crystal phase	Temp. (°C)	Reduction duration (h)	Crystal phase
Sample A					
120	15	Poorly crystalline			
250	10	$Fe_2(MoO_4)_3$	400	12	β-$FeMoO_4$, MoO_3, $Fe_2(MoO_4)_3$ minor
			600	5	MoO_2, β-$FeMoO_4$
400	10	$Fe_2(MoO_4)_3$, MoO_3	373	12	MoO_2, β-$FeMoO_4$
			450	12	MoO_2, $FeMoO_3$, β-$FeMoO_4$
			600	12	MoO_2, $FeMoO_3$, Mo
			600	50	Mo, MoO_2, (trace)
600	10	$Fe_2(MoO_4)_3$, MoO_3	600	50	MoO_2, Mo, $FeMoO_3$
Sample B					
400	10	Fe_2O_3, MoO_3	600	50	Mo, Fe

of the sample at 400 °C, the $Fe_2(MoO_4)_3$ phase remains unchanged on further heating of the sample up to 600 °C.

The IR spectra of the precipitated mass, heat-treated at 120, 250 and 400 °C are shown in Fig. 2. the IR spectra at 120 and 250 °C are nearly identical. Only the intensity of the IR band at 860 cm^{-1} increases at 250 °C. However, some new bands at 980, 400, 370 and 350 cm^{-1} appear on the heat treatment of the sample at 400 °C. The IR spectrum of pure MoO_3 obtained by the decomposition of $(NH_4)_6\ Mo_7O_{24} \cdot 4\ H_2O$ is also shown in Fig. 2D.

Reduction

The reduction of the oxide mass was carried out under a hydrogen atmosphere (50 ml min^{-1}). To examine the effect of calcination temperature on the reduction process, sample A was calcined up to three different temperatures, namely 250, 400 and 600 °C, before starting the reduction. The DSC curves under hydrogen are shown in Fig. 3.

The DSC curve for the sample precalcined at 250 °C (Fig. 3A) shows only a very weak exotherm at 335 °C, which is followed by a broad endothermic peak with a maximum at 590 °C. The DSC curve is quite different for the sample precalcined at 400 °C (Fig. 3B). It shows two exotherms with maxima at 455 and 490 °C followed by a strong endotherm at 605 °C. The DSC curve is similar in nature if the sample is precalcined at 600 °C (Fig. 3C), but the peak maxima are shifted to higher temperatures.

The nature of the reduction of a mechanical mixture of iron and molybdenum oxides and pure molybdenum oxide are shown in Fig. 4. The

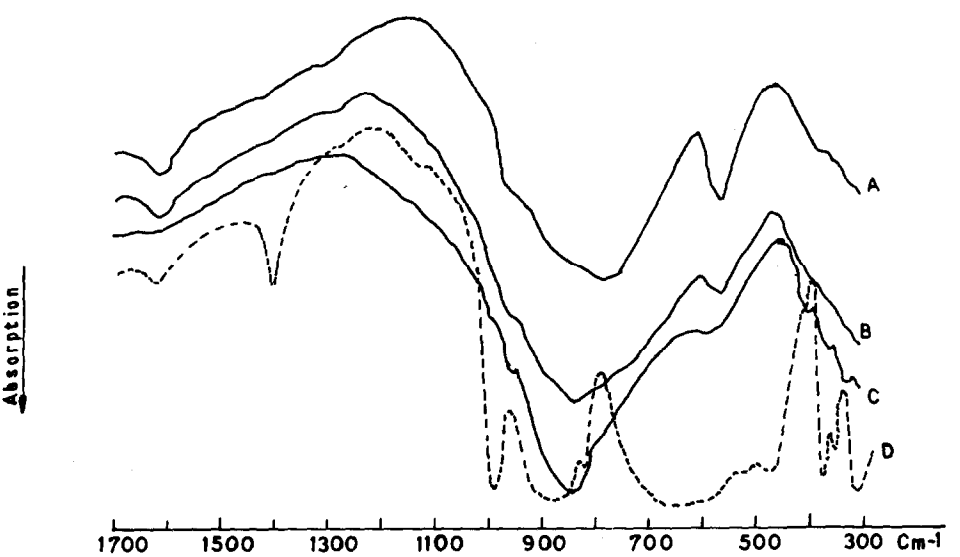

Fig. 2. IR spectral bands of the precipitated mass calcined at different temperatures. (A) 120 °C; (B) 250 °C, (C) 400 °C, (D) pure MoO_3.

nature of the DSC curve for a precipitated sample is quite similar to that of a mechanical mixture except for the presence of one weak endothermic peak at 495 °C. However, the peak maxima in the case of a mechanical mixture lie at higher temperatures (Fig. 4B). The reduction of MoO_3 also shows two exotherms at 505 and 570 °C and an endothermic peak at 645 °C. The DSC curve also shows a weak exotherm at 380 °C.

The crystal phase composition of precipitated samples after reduction at different temperatures is shown in Table 1. XRD studies indicate that MoO_2 and $FeMoO_4$ are formed as major phases at the initial stage of reduction. The MoO_2 phase exists up to 575 °C, but $FeMoO_4$ reduces to $FeMoO_3$ above

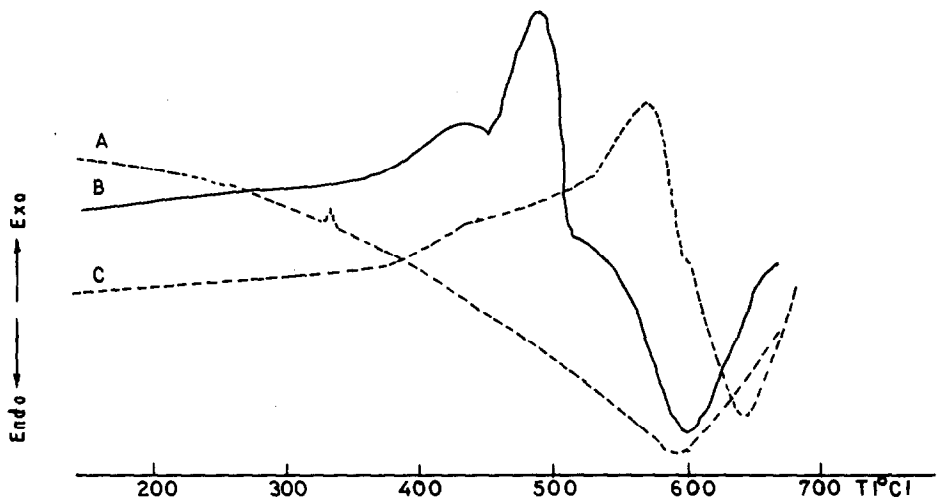

Fig. 3. DSC curves of the precipitated mass under hydrogen atmosphere. (A) Calcined at 250 °C, (B) calcined at 400 °C, (C) calcined at 600 °C.

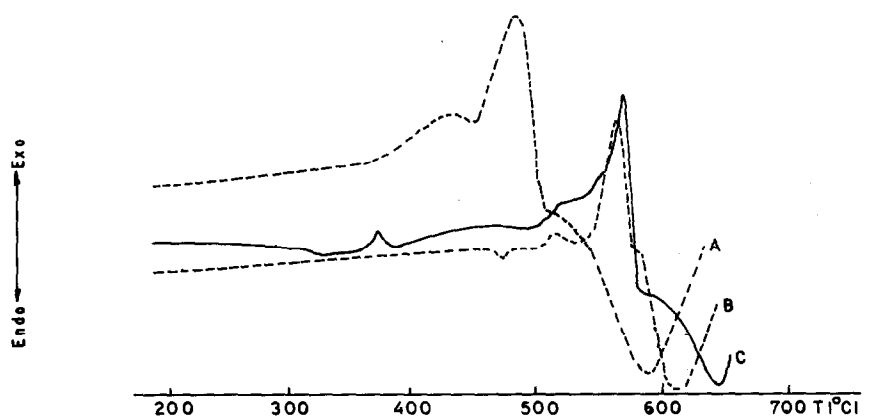

Fig. 4. DSC curves of the samples under hydrogen atmosphere. (A) Precipitated iron–molybdenum mixed oxides calcined at 400 °C, (B) mechanical mixture of Fe_2O_3 and MoO_3, (C) pure MoO_3.

450 °C. XRD patterns indicate mostly an elemental molybdenum phase on reducing the sample at 600 °C for 50 h along with a very small amount of the MoO_2 phase. The reduction remains more incomplete at 600 °C if the sample is precalcined at 600 °C as indicated by the presence of more of the MoO_2 phase. No elemental iron phase was detected in XRD patterns after reduction in the case of sample A. However, the formation of two separate phases consisting of elemental iron and molybdenum was detected in XRD patterns on reducing sample B at 600 °C for 50 h.

The interaction of a synthesis gas mixture ($P^0_{H_2} = 6.0$ bar; $P^0_{CO} = 3.9$ bar) with the reduced oxide masses was examined in a high pressure DSC cell. The reduced mass obtained from the mechanical mixture shows a strong exotherm with a starting temperature at 290 °C (Fig. 5B). The exothermic peak is a doublet with a hump at 355 °C, which is absent in the two other samples (Fig. 5B,C). In the case of pure elemental molybdenum, the exothermic reaction starts above 370 °C and the exotherm is also weaker. In the case of the precipitated sample, the exothermic reaction starts above 230 °C. Activation energies were calculated for the exothermic process with the help of a computer-fit program (Active I and II) from the Arrhenius plot of evolved heat against T^{-1} (K).

DISCUSSION

Dehydration of the precipitated oxide mass is complete below 300 °C. Two endothermic peaks below 300 °C can be assigned for the removal of adsorbed water and coordinated water molecules. Thermogravimetric mea-

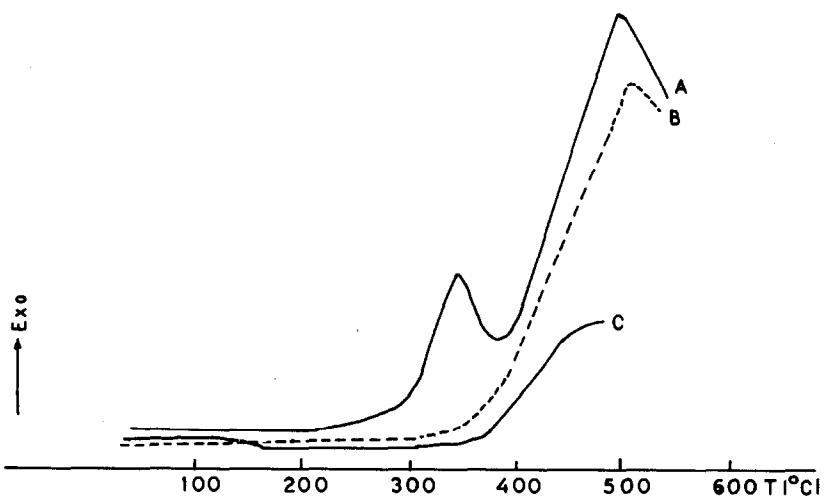

Fig. 5. DSC curves of the reduced mass under synthesis gas mixture ($CO + H_2$). (A) Reduced mass obtained from sample A (precipitated), (B) reduced mass obtained from mechanical mixture of Fe_2O_3 and MoO_3, (C) reduced MoO_3.

surements indicate that there is no weight loss above 300 °C, which supports a complete dehydration of the precipitated mass by 300 °C. The XRD pattern also indicates the formation of the $Fe_2(MoO_4)_3$ phase after calcination at 250 °C.

The exothermic peak at 373 °C in the DSC curve can be assigned to the separation of the MoO_3 phase from the polymolybdate ions, which are formed during precipitation. The formation of polymeric molybdenum octahedra, like $Mo_7O_{24}^{6-}$ ions during the precipitation, was also reported in earlier works [20–22], especially if the molarity of the solution is high and precipitation is carried out at the lower pH range of ~ 2.

This polymeric species yielded MoO_3 on calcining the precipitated mass above 350 °C, and ordering in the $Fe_2(MoO_4)_3$ lattice is attained by the removal of excess MoO_3. The exothermic peak is a doublet in nature as the two processes occur simultaneously. Trifiro et al. [23] reported the crystallization of the amorphous $Fe_2(MoO_4)_3$ phase. However, some discrepancies in peak intensities for a pure $Fe_2(MoO_4)_3$ phase can be accounted for by the presence of incorporated polymolybdate ions. It seems more appropriate, therefore, to consider this exothermic process as lattice ordering rather than as a simple crystallization process. The XRD pattern also indicates that the separation of the MoO_3 phase only occurs at 400 °C. Both the MoO_3 and $Fe_2(MoO_4)_3$ phases are observed in XRD patterns at 400 and 600 °C. $Fe_2(MoO_4)_3$ remains stable up to 600 °C. Bhattacharya et al. [24] reported the dissociation of $Fe_2(MoO_4)_3$ into α-Fe_2O_3 and MoO_3 above 350 °C. In the present study no separate α-Fe_2O_3 phase was noticed during the calcination process under argon. However, the preparative method adopted in the present study is not identical to that followed by Bhattacharya et al. Possibly the presence of excess MoO_3 in the $Fe_2(MoO_4)_3$ lattice, as polymolybdate, inhibits the separation of any α-Fe_2O_3 phase. IR spectroscopic studies support the separation of only the MoO_3 phase at 400 °C (Fig. 2). IR spectral bands can be assigned for the formation of an $Fe_2(MoO_4)_3$ lattice even on calcining the sample at 250 °C [25].

On calcination at 250 °C, the sample consists of an $Fe_2(MoO_4)_3$ phase contaminated with polymolybdenum ions as confirmed by X-ray diffraction results. DSC results indicate that the reduction of $Fe_2(MoO_4)_3$ is endothermic in nature and proceeds slowly as indicated by a very borad endothermic peak with a maximum at 595 °C. The separation of free MoO_3 from polymolybdate is not favourable under an H_2 atmosphere as only a very weak exothermic peak is observed during heat treatment under H_2 (Fig. 3A). The presence of polymeric molybdenum octahedra makes the reduction process more difficult [20]. The reduced sample consists of the $FeMoO_4$ and MoO_2 phases even at 600 °C as confirmed from the XRD pattern (Table 1).

However, on calcining the sample at 400 °C, the MoO_3 phase is separated completely and the $Fe_2(MoO_4)_3$ lattice becomes free from polymeric molybdenum octahedra. The reduction process becomes exothermic in na-

ture as indicated by the two exothermic peaks (Fig. 3B). These exothermic peaks can be assigned to the transformation of the MoO_3 phase into the MoO_2 state through other intermediate oxides (MoO_{3-x}). This assignment is confirmed by comparing the curve (Fig. 4C) which consists of only the MoO_3 phase. The peak maxima are lower in the earlier case, which can be ascribed to the formation of the MoO_3 phase over the $Fe_2(MoO_4)_3$ surface as small crystallites during the calcination process.

The stepwise reduction of the MoO_3 phase in the case of the supported catalyst was also reported by Thomas et al. [26]. The reduction of the $Fe_2(MoO_4)_3$ phase occurs simultaneously, which is endothermic in nature as discussed earlier. An overall exothermic effect has been noticed, however, due to the strong exothermic process for the reduction of the MoO_3 phase into the MoO_2 state. The further reduction of the MoO_2 phase is endothermic in nature, as indicated by the presence of a strong endothermic peak at 610 °C. The last endothermic process is related to the formation of elemental molybdenum through the reduction of the MoO_2 and $FeMoO_3$ phases. The reduction of MoO_2 to elemental molybdenum possibly occurs through other intermediate oxides (MoO_{2-x}) as some extra diffraction lines were observed in the XRD patterns. However, it is difficult to assign the formation of any definite intermediate oxides from X-ray diffraction studies. On reducing the precipitated sample at 600 °C, the residual mass consists of a single Mo phase with a cubic lattice (Table 1). No separate elemental iron or iron oxide phase has been observed. The results indicate that the reduction of $FeMoO_3$ produces a mixed crystal of iron and molybdenum [16,17]. The XRD patterns, however, do not indicate the formation of any definite stoichiometric Fe_xMo alloy in the present study, which is possibly related to the presence of a low concentration of iron in the mixed oxide precipitate. Elemental iron remains in a dispersed state in the molybdenum lattice. Mössbauer spectroscopic studies also do not indicate the formation of any metallic iron phase for the reduced catalyst. The measured lattice parameter value for the molybdenum phase, $a_0 = 3.124$ Å is lower than that of pure elemental molybdenum ($a_0 = 3.147$ Å). This decrease in the lattice parameter value may be assigned to the incorporation of elemental iron in the molybdenum lattice without altering the crystal symmetry.

In the case of the mechanical mixture, the reduction is more simple. The formation of both elemental iron and molybdenum phases are noticed in the XRD pattern at 600 °C (Table 1). The measured lattice parameter values ($a_0 = 2.86$ Å for elemental iron and $a_0 = 3.14$ Å for elemental molybdenum) are in good agreement for the existence of both lattices in the pure state. The DSC curve also shows that the nature of the reduction of MoO_3 is unaffected by the presence of the elemental iron phase. The formation of the elemental molybdenum phase, however, occurs at a lower temperature, which was also noticed by earlier workers [17,18]. The formation of elemental molybdenum occurs at still lower temperatures in case of the precipitated sample, which is

possibly related to the higher surface area and lower crystallite size of the MoO_3 phase ($d = 10$ nm). Crystallite size measurements indicate that the elemental molybdenum phase formed by reduction remains in a poorly crystalline state in both samples A and B.

Hydrogenation of CO over reduced samples

The DSC curves (Fig. 5) show that elemental molybdenum is not very active for the hydrogenation of CO. The measured activation energy, $E = 241$ kJ mol^{-1}, is also highest in the case of the sample consisting of only the elemental molybdenum phase. The activation energy is lowest (130 kJ mol^{-1}) for the sample consisting of iron–molybdenum mixed oxide prepared by simple mechanical mixing (sample B). The activation energy is comparatively higher (160 kJ mol^{-1}) for the mixed oxide prepared by the precipitation method (sample A).

Product gas analysis by the gas chromatographic method indicates the formation of mostly low carbon-number paraffins (CH_4, C_2H_6, C_3H_8) after the synthesis reaction. The catalytic activity of $Fe_2(MoO_4)_3$ has also been verified in an isothermal metal block reactor with the same gas composition used in the present study [27]. Product analysis supports the formation of mostly CH_4 and C_2H_6 and a very low C_{5+} fraction at 330 °C and 11 bar. Structural studies indicate that elemental molybdenum is stable under synthesis conditions, but in the case of sample B, which consists of a mixture of elemental iron and molybdenum in a reduced state, reacts with synthesis gases and an iron carbide phase is formed during the synthesis process. In the case of sample A, no iron carbide phase is formed as confirmed from XRD patterns. The results can be ascribed to the presence of elemental iron as a mixed crystal within the molybdenum lattice and the chance of the formation of a carbide phase is diminished. A higher catalytic activity was reported for supported molybdenum catalysts [5–7] which also consist of alkali promoters [1–5]. The results may be due to the catalytic activity of the elemental molybdenum phase being enhanced by the incorporation of alkali promoters. The incorporation of elemental iron into the molybdenum catalyst by simple mechanical mixing is not very useful for producing a stable catalyst, since the carburization of elemental iron occurs readily under synthesis conditions, which is a deactivation step for a Fischer–Tropsch synthesis. However, a mixed lattice consisting of elemental iron and molybdenum is formed in the case of sample A, which seems to be more stable under synthesis conditions. However, the sample is active only above 300 °C. Further work is necessary to evaluate the correct ratio of Fe and Mo which may be active at lower temperatures, for a Fischer–Tropsch synthesis reaction to be carried out.

CONCLUSION

A mixed crystal catalyst consisting of iron and molybdenum can be obtained by hydrogen reduction of precipitated $Fe_2(MoO_4)_3 \cdot x\ H_2O$. The reduced mass is active for the hydrogenation of CO, and stable towards the carburization process.

REFERENCES

1 R.B. Anderson, in P.H. Emmett (Ed.), Catalysis, Vol. IV, Reinhold, New York, 1956.
2 R.J. Madon and H. Shaw, Catal. Rev. Sci. Eng., 15 (1977) 69.
3 H. Pichler, Adv. Catal., 4 (1952) 271.
4 C.H. Bartholomew and J.R. Katzer, Catalysis Deactivation, Elsevier, Amsterdam 1980, p. 375.
5 J. Sebastian, Carnegie Inst. Technol., Coal Res. Lab. Contrib., 35 (1936) 8.
6 S.G. Stewart, U.S. Patent, 2490.488 (1949).
7 C.B. Murchison and D.A. Murdick, I.T.A., 0016852 (1979).
8 C.B. Murchison and D.A. Murdick, Hydrocarbon Process., 60 (1981) 159.
9 H.J. Krebs, H.P. Bonzel and W. Schwarting, J. Catal., 72 (1981) 199.
10 M.E. Dry, T. Shingles and L.J. Boshoff, J. Catal., 25 (1972) 99.
11 M. Carbucicchio and F. Trifiro, J. Catal., 45 (1976) 77.
12 P. Jiru, B. Wichterlowa and J. Tichy, Proc. 3rd Int. Congr. Catal., Amsterdam, 1964, p. 199.
13 N. Barriesci, F. Garbassi, M. Petrera and G. Petrini, Catalysis Deactivation, Elsevier, Amsterdam, 1980, p. 115.
14 P. Forzatti, P.L. Villa, N. Ferlazzo and D. Jones, J. Catal., 76 (1982) 188.
15 F. Trifiro, V. de Vecchi and I. Pasquon, J. Catal., 15 (1969) 8.
16 V.E. Thachenko, A.V. Gurev and M.V. Slinkina, Zh. Prikl. Khim., 52 (1979) 36.
17 A.S. Grintsov, Chem. Abstr., 87 26550a.
18 Yu.A. Pavlov, V.A. Polyakov and V.V. Ploshkin, Chem. Abstr., 88 108619q.
19 Index to the Powder Diffraction File, American Society for Testing Materials, 1967.
20 P. Ratnasamy and S. Sivasanker, Catal. Rev. Sci. Eng., 22 (1980) 401.
21 H. Knozinger and R. Jeriorowski, J. Phys. Chem., 82 (1978) 2002.
22 M. Lojacono, J.L. Verbeek and G.C.A. Schuit, J. Catal., 29 (1973) 463.
23 F. Trifiro, P. Centola and I. Pasquon, Proc. Int. Symp. Heterogeneous Catalysts, Elsevier, Amsterdam, 1975, p. 151.
24 P.K. Bhattacharya, P.P. De, R. Jaganattian and S.K. Bhattacharya, Indian J. Chem., 14 (1976) 973.
25 F. Trifiro, S. Notarbartolo and I. Pasquon, J. Catal., 22 (1971) 324.
26 R. Thomas, V.H.J. de Beer and J.A. Moulijr, Bull. Soc. Chim. Belg., 90 (1981) 1349.
27 R. Malessa, unpublished work, 1981.